International Journal of Nanomedicine

Dovepress
open access to scientific and medical research

Open Access Full Text Article

ORIGINAL RESEARCH

Oral Delivery of Anti-Parasitic Agent-Loaded PLGA Nanoparticles: Enhanced Liver Targeting and Improved Therapeutic Effect on Hepatic Alveolar Echinococcosis

Jun Li[1,*], Yangyang Yang[2,*], Xiumin Han[3,*], Jing Li[2], Mengxiao Tian[1], Wenjing Qi[1], Huniu An[3], Chuanchuan Wu[1], Yao Zhang[1], Shuai Han[4], Liping Duan[4], Weisi Wang[4], Wenbao Zhang[1]

[1]State Key Laboratory of Pathogenesis, Prevention and Treatment of High Incidence Diseases in Central Asia, Clinical Medical Research Institute, the First Affiliated Hospital of Xinjiang Medical University, Urumqi, Xinjiang, People's Republic of China; [2]Shanghai Key Laboratory of Chemical Biology, School of Pharmacy, East China University of Science and Technology, Shanghai, People's Republic of China; [3]Qinghai Provincial People's Hospital, Xining, Qinghai, People's Republic of China; [4]NHC Key Laboratory of Parasite and Vector Biology, WHO Collaborating Centre for Tropical Diseases, National Institute of Parasitic Diseases, Chinese Center for Disease Control and Prevention, Shanghai, People's Republic of China

*These authors contributed equally to this work

Correspondence: Wenbao Zhang; Weisi Wang, Tel +86 991 4366319; +86 21 64377008, Email wenbaozhang2013@163.com; wangws@nipd.chinacdc.cn

International Journal of Nanomedicine downloaded from https://www.dovepress.com/ on 08-Jun-2023
For personal use only.

Background: Alveolar echinococcosis (AE) is a lethal parasitic disease caused by infection with the metacestode of the dog/fox tapeworm *Echinococcus multilocularis*, which primarily affects the liver. Although continued efforts have been made to find new drugs against this orphan and neglected disease, the current treatment options remain limited, with drug delivery considered a likely barrier for successful treatment.

Methods: Nanoparticles (NPs) have gained much attention in the field of drug delivery due to their potential to improve delivery efficiency and targetability. In this study, biocompatible PLGA nanoparticles encapsulating a novel carbazole aminoalcohol anti-AE agent (H1402) were prepared to promote the delivery of the parent drug to liver tissue for treating hepatic AE.

Results: H1402-loaded nanoparticles (H1402-NPs) had a uniform spherical shape and a mean particle size of 55 nm. Compound H1402 was efficiently encapsulated into PLGA NPs with a maximal encapsulation efficiency of 82.1% and drug loading content of 8.2%. An in vitro uptake assay demonstrated that H1402-NPs rapidly penetrated the in vitro cultured pre-cyst wall and extensively accumulated in the pre-cysts of *E. multilocularis* within only 1 h. The biodistribution profile of H1402-NPs determined through ex vivo fluorescence imaging revealed significantly enhanced liver distribution compared to unencapsulated H1402, which translated to improved therapeutic efficacy and reduced systemic toxicity (especially hepatotoxicity and cytotoxicity) in a hepatic AE murine model. Following a 30-day oral regimen (100 mg/kg/day), H1402-NPs significantly reduced the parasitic burden in both the parasite mass (liver and metacestode total weight, 8.8%) and average metacestode size (89.9%) compared to unmedicated infected mice (both p-values < 0.05); the treatment outcome was more effective than those of albendazole- and free H1402-treated individuals.

Conclusion: Our findings demonstrate the advantages of encapsulating H1402 into PLGA nanoparticles and highlight the potential of H1402-NPs as a promising liver-targeting therapeutic strategy for hepatic AE.

Keywords: alveolar echinococcosis, *Echinococcus multilocularis*, PLGA, nanoparticles, liver targeting, oral administration

Introduction

Human alveolar echinococcosis (AE) is a life-threatening parasitic disease caused by infection with the larval form (metacestode) of the dog/fox tapeworm *Echinococcus multilocularis*. Human AE is considered an orphan and neglected disease by the World Health Organization. AE is endemic in the northern hemisphere, especially in Eurasia.[1] The current estimate of the global burden of human AE is 687,823 disability-adjusted life years (DALYs).[2] Most cases of AE occur in

Received: 14 November 2022
Accepted: 26 May 2023
Published: 8 June 2023

© 2023 Li et al. This work is published and licensed by Dove Medical Press Limited. The full terms of this license are available at https://www.dovepress.com/terms.php and incorporate the Creative Commons Attribution – Non Commercial (unported, v3.0) License (http://creativecommons.org/licenses/by-nc/3.0/). By accessing the work you hereby accept the Terms. Non-commercial uses of the work are permitted without any further permission from Dove Medical Press Limited, provided the work is properly attributed. For permission for commercial use of this work, please see paragraphs 4.2 and 5 of our Terms (https://www.dovepress.com/terms.php).

Graphical Abstract

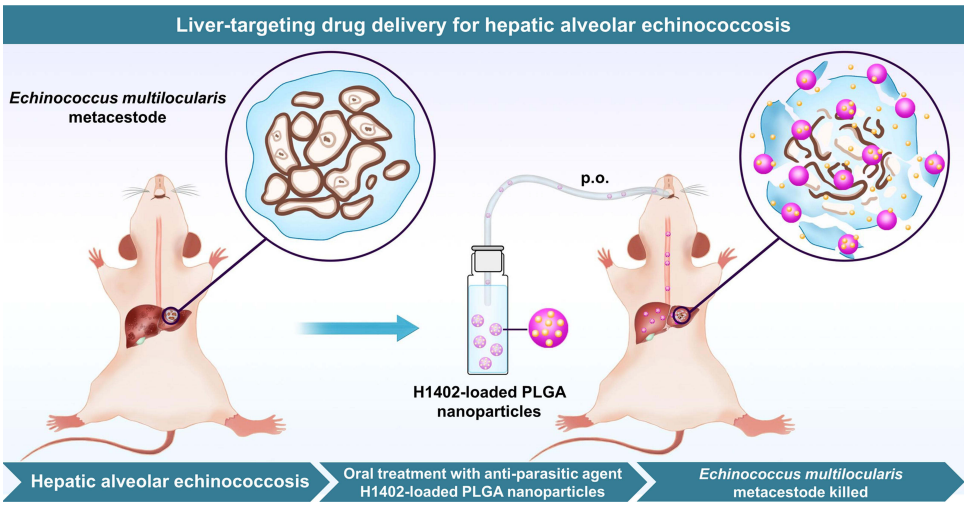

China, with an estimated 34,000 cases during 2012–2016.[3] A total of 115 counties in China are considered to be AE-endemic, and are predominantly distributed in the Qinghai-Tibetan Plateau, with a human prevalence of ≥ 5% in some local communities.[1,3–5] In Europe, AE is the top-ranked foodborne parasitic disease and shows an increasing trend in human incidence in some previously recognized endemic areas, despite the relatively small case numbers reported.[2,6,7]

The natural life cycle of *E. multilocularis* typically involves canids (mostly foxes and dogs) as definitive hosts and small mammals (often rodents) as intermediate hosts. Humans are accidental hosts who become infected through the ingestion of the worm eggs shed with the feces of definitive hosts. A typical feature of AE is a tumor-like aggressive proliferation of the metacestodes, affecting the liver in nearly 100% of cases. This metacestode proliferation not only infiltrates the adjacent host tissues to form pseudocystic lesions, but also forms metastases in distant organs, with massive periparasitic infiltrate of host's cells and fibrosis.[8] The 10-year mortality of AE is thought to be > 90% without proper treatment.[9]

Radical resection of the parasitic mass by surgical intervention is the gold standard therapy for AE. However, complete removal of parasitic lesions is usually not feasible due to the infiltrative nature and/or complicated lesion location of the metacestode tissue.[1,10] For inoperable cases, albendazole-based anti-parasitic treatment remains the only option. However, albendazole shows low oral bioavailability, restricted uptake by the metacestodes, and, most importantly, only has parasitistatic but not parasiticidal effects in patients with AE; hence, it requires life-long administration at massive doses to avoid recurrence.[11–13] The long-term and high-dose regimens of albendazole are not always well tolerated and can have severe adverse effects (eg, hepatotoxicity) in patients suffering from AE.[10,14] Therefore, alternative anti-AE drugs are urgently required.

We previously identified an orally bioavailable novel anti-echinococcal agent termed compound H1402, which is characterized by a distinctive carbazole aminoalcohol scaffold (Figure 1).[15,16] Compound H1402 was found to exhibit excellent therapeutic efficacy against cystic echinococcosis (CE; another form of human echinococcosis caused by infections of *Echinococcus granulosus sensu lato*) both in vitro and in vivo.[15] However, the anti-parasitic potency of H1402 was declined for the more aggressive and complicated echinococcosis-AE,[16] probably due to inadequate drug exposure in the parasite lesion. Therefore, a new drug delivery system with improved targeting capacity of the most affected organ, the liver, is urgently required to increase drug exposure and address this clinical issue.

Poly (lactic-co-glycolic acid) (PLGA), which has good biodegradability and is non-immunogenic, has been approved as a drug nanocarrier by both the US Food and Drug Administration and the European Medicines Agency. Moreover, PLGA-based drug delivery systems have shown broad compatibility with different routes of administration, including

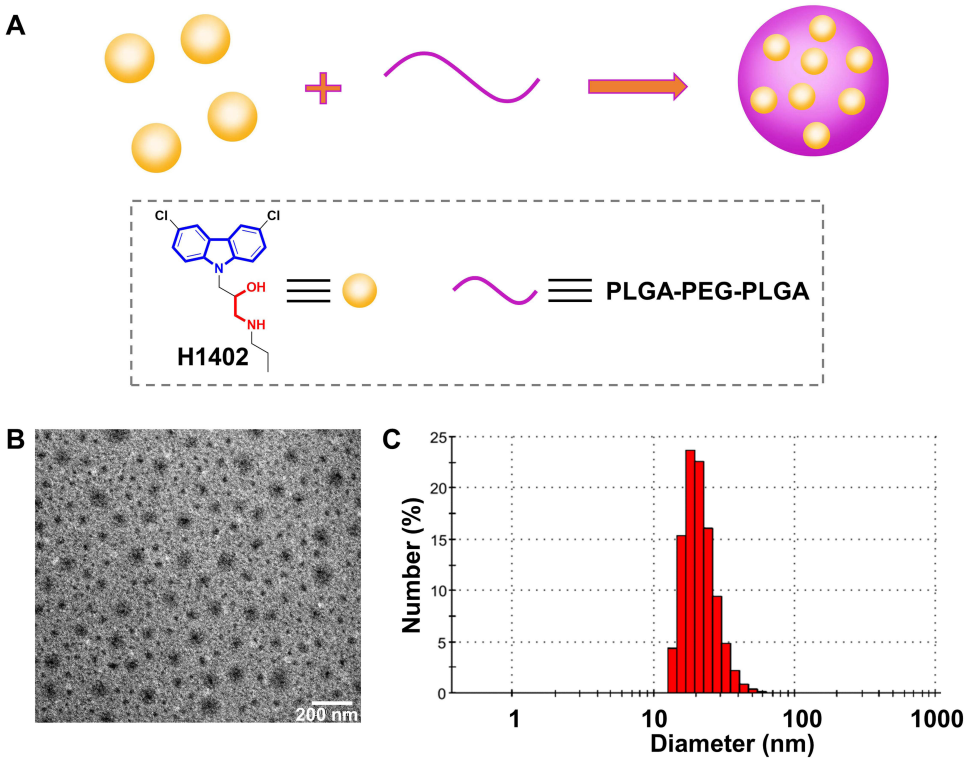

Figure 1 Schematic representation of the encapsulation of carbazole aminoalcohol anti-echinococcal agent-compound H1402 into PLGA-PEG-PLGA polymers to produce H1402 nanoparticles (**A**). Transmission electron microscopy micrograph (**B**) and particle size distribution (**C**) of H1402 nanoparticles.

intravenous injection and oral delivery, both of which exhibit excellent hepatic targeting capacity and have been widely applied, particularly for the treatment of liver disease.[17–19] Considering that the liver is the organ most affected by AE, it is expected that encapsulating compound H1402 with PLGA nanoparticles will increase the accumulation of the drug in the liver and improve the therapeutic effect.

In the current study, in order to promote the liver targetability of the anti-echinococcal agent H1402 and improve its parasiticidal potency, the H1402-loaded PLGA nanoparticles (H1402-NPs) were prepared. The biodistribution profile of the H1402-NPs was determined through ex vivo fluorescence imaging. The therapeutic efficacy of the H1402-NPs against *E. multilocularis* infections was then evaluated in a hepatic AE mouse model. The pharmacokinetic and safety profiles of H1402-NPs are also described in this report.

Materials and Methods

Materials

Compound H1402 (1-(3,6-dichloro-9*H*-carbazol-9-yl)-3-(propylamino)propan-2-ol) was synthesized in-house as previously described.[15] D, L-lactide (LA), glycolide (GA), cyanine 5.5 (Cy5.5) carboxylic acid (Cat# C854973), 2-(1*H*-benzotriazole-1-yl)-1,1,3,3-tetramethyluronium hexafluorophosphate (HBTU, Cat# H810969), 1-hydroxybenzotriazole (HOBT, Cat# H810970), and *N, N*-diisopropylethylamine (DIPEA, Cat# N807281) were purchased from Shanghai Macklin Biotechnology Co., Ltd. (Shanghai, China); polyethylene glycol (PEG, MW = 1000) and stannous 2-ethylhexanoate were purchased from Shanghai Yien Chemical Technology Co., Ltd. (Shanghai, China); dialysis membrane (MW = 3500) was purchased from Nantong Feiyu Biotechnology Co., Ltd. (Nantong, China); Solutol HS-15 (Cat# K487242) and hydroxypropyl-β-cyclodextrin (Cat# H476639) were purchased from Shanghai Aladdin Biochemical Technology Co., Ltd. (Shanghai, China); and the human HepG2 cell line (Cat# SCSP-510) was obtained from the Cell Bank of the Type Culture Collection of the Chinese Academy of Sciences.

Synthesis of PLGA-PEG-PLGA Polymers

PEG (10.0 g, 10.0 mM) was added to a dry two-necked flask and stirred at 150°C for 3 h under the protection of argon. Subsequently, GA (4.9 g, 42.3 mM) and LA (18.4 g, 128.0 mM) were added. After melting of the monomers, the catalyst, stannous 2-ethylhexanoate (0.1 g, 0.3 mM), was added; the flask was replaced with argon three times to remove the air and stirred at 150°C for 12 h (Figure S1). The ^{1}H NMR (400 MHz, AVANCE III 400, Bruker Corporation, Switzerland) and FT-IR (400–4000 cm^{-1}, Nicolet 6700, Thermo Fisher Scientific Inc., Waltham, MA, USA) spectra of PLGA-PEG-PLGA polymers were recorded to confirm the conjugation (Figure S2).

Preparation and Characterization of H1402-NPs

The obtained PLGA-PEG-PLGA polymers were used as carrier materials to prepare H1402-loaded nanoparticles (termed as H1402-NPs). Compound H1402 (20 mg) was dissolved in dimethyl sulfoxide (DMSO, 2 mL) before being added to a solution of PLGA-PEG-PLGA polymers (500 mg) in deionized water. The mixture was stirred at 4°C overnight, before dialyzing against deionized water through a dialysis membrane (MW: 3500 cut-off) for 5 days to remove the unencapsulated H1402.

The particle size distribution and chargeability of the obtained H1402-NPs were determined using dynamic light scattering (DLS; Dynapro Titan TC, Malvern Panalytical Ltd., Malvern, United Kingdom). The morphology of PLGA nanoparticles was observed using transmission electron microscopy (TEM; JEM-2100, JEOL, Tokyo, Japan). H1402-NPs were placed on a carbon film-coated copper grid, stained with phosphotungstic acid (1.0% w/v), and dried in air before visualization.

Loading Content and Encapsulation Efficiency of H1402-NPs

H1402-NPs were dissolved in DMSO and sonicated for 10 min to collapse the nanoparticle structure. The absorption of the solution at 303 nm was measured using the Nanodrop 2000 (Thermo Fisher Scientific, Waltham, MA, USA) at 303 nm, and the concentration of free H1402 was obtained using the linear equation: $y = 3.82071x + 0.00618$, $R^2 = 0.9983$ (Figure S3). The loading content (LC) and encapsulation efficiency (EE) of H1402 in nanoparticles were calculated as follows:

$$\text{Loading content } (\%) = \frac{\text{weight of encapsulated nanodrug}}{\text{total weight of NPs}} \times 100\%$$

$$\text{Encapsulation efficiency } (\%) = \frac{\text{weight of encapsulated nanodrug}}{\text{total weight of nanodrug}} \times 100\%$$

Preparation of Cy5.5-Labeled H1402 and Cy5.5-H1402 Nanoparticles

Cy5.5 carboxylic acid (500 mg, 807 μM), HBTU (398 mg, 1.05 μM), and HOBT (142 mg, 1.05 μM) were dissolved in dry dimethylformamide (DMF, 150 mL) and stirred at room temperature under the protection of argon for 10 min. Subsequently, DIPEA (242 μL, 1.37 mM) was added and stirred for another 10 min. Next, a DMF solution (70 mL) of compound H1402 (284 mg, 807 μM) was added and the reaction mixture was stirred for 24 h in darkness. After reaction, the mixture was concentrated in a vacuum, and the obtained residues were purified using column chromatography (CH_2Cl_2:MeOH = 100:1–10:1) to afford the target compound Cy5.5-H1402 [2-((1*E*,3*E*,5*E*)-5-(3-(6-((3-(3,6-dichloro-9*H*-carbazol-9-yl)-2-hydroxypropyl)(propyl) amino)-6-oxohexyl)-1,1-dimethyl-1,3-dihydro-2*H*-benzo[*e*]indol-2-ylidene)penta-1,3-dien-1-yl)-1,1,3-trimethyl-1*H*-benzo[*e*]indol-3-ium chloride]. Dark blue glossy solid, yield: 71%. ^{1}H NMR (400 MHz, $CDCl_3$) δ 8.04 (d, J = 8.5 Hz, 2H, Ar-H), 7.98–7.77 (m, 8H, Ar-H and CH), 7.52 (t, J = 7.6 Hz, 2H, Ar-H), 7.47–7.21 (m, 8H, Ar-H and CH), 6.58 (t, J = 12.3 Hz, 1H, CH), 6.08 (t, J = 14.0 Hz, 2H, CH_2), 4.53 (s, 1H, OH), 4.25–4.18 (m, 2H, 2CH), 4.00–3.97 (m, 2H, CH_2), 3.70–3.58 (m, 1H, CH), 3.55 (s, 3H, CH_3), 3.12–3.04 (m, 2H, CH_2), 2.31 (t, J = 6.8 Hz, 2H, CH_2), 1.90 (d, J = 5.7 Hz, 12H, 4CH_3), 1.79–1.75 (m, 2H, CH_2), 1.67–1.63 (m, 2H, CH_2), 1.45–1.43 (m, 2H, CH_2), 1.32–1.18 (m, 4H, 2CH_2), 0.69 (t, J = 7.3 Hz, 3H, CH_3). HPLC (220 nm): t_R = 4.8 min, purity: 98.5%. The Cy5.5-H1402 nanoparticles (Cy5.5-H1402-NPs) were prepared in the same manner as described in the section of Preparation and characterization of H1402-NPs.

Isolation of *E. multilocularis* Protoscoleces and in vitro Culture of *E. multilocularis* Metacestodes

The *E. multilocularis* Xinjiang strain was maintained and propagated in the peritoneum of Kunming mice. Six months after intraperitoneal inoculation with *E. multilocularis* protoscoleces, the mice were euthanized and the *E. multilocularis* metacestode material was recovered aseptically from the peritoneal cavity. The parasite material was washed three times with phosphate-buffered saline (PBS), before mincing and grinding. The homogenized metacestode material was diluted with PBS to obtain a 1:5 suspension, which was first sieved through a sterile gauze, before filtering the flow through using a 70-mesh nylon mesh. After natural settlement, the protoscoleces were digested with 1.0% of pepsin in Hank's solution at pH 2.0 for 30 min, and then washed five times with PBS containing antibiotics (100 IU/mL of penicillin and 100 μg/mL of streptomycin [Cat# 15140122, HyClone, Logan, UT, USA]) under aseptic conditions. The protoscoleces viability was assessed with 0.1% methylene blue. Protoscoleces with > 95% viability were cultured in RPMI 1640 culture medium (Cat# SH30809.01, HyClone, Logan, UT, USA) supplemented with 20% fetal calf serum (Cat# 10099148, Gibco, Penrose, New Zealand) and antibiotics at 37°C in 5% CO_2. The culture medium was changed every 5 days. In vitro cultured pre-cysts (less than four weeks, diameter: 200–300 μm) were used for uptake assay, and fully developed metacestodes (4–6 months) were used for in vitro parasiticidal assay when they reached 4–6 mm in diameter.

Pre-Cyst Uptake Assay

In vitro cultured pre-cysts were maintained in a 24-well plate (10 pre-cysts/well) as described in the section of Isolation of *E. multilocularis* protoscoleces and in vitro culture of *E. multilocularis* metacestodes. Cy5.5-H1402-NPs were applied to the pre-cysts in each well at a concentration of 20 μM for 12 h. At scheduled time points (0.5, 1, 3, 6, and 12 h post-treatment), the pre-cysts were collected and rinsed with PBS thrice, before observing with an inverted fluorescence microscope (IX73, Olympus Corporation, Tokyo, Japan). The experiments were performed in triplicate.

Cytotoxicity Assay

The cytotoxicity of free H1402 and H1402-NPs against human HepG2 cells was investigated through measuring the cell viability using the CCK-8 assay. Briefly, HepG2 cells were seeded in 96-well plates at a density of 5×10^3 cells/well. Cells were treated with free H1402 or H1402-NPs at corresponding final concentrations (H1402: 10, 20, 25, 30, 40, and 50 μM; H1402-NPs: 10, 25, 50, 60, 70, 80, and 100 μM) for 48 h at 37°C in 5% CO_2. Control cells received the vehicle (DMSO, 0.1% v/v or deionized water) only. The cell viability was measured using the Cell Counting Kit-8 (Cat# C0038, Beyotime Biotechnology Co., Ltd., Shanghai, China) according to the manufacturer's instructions.

In vitro Parasiticidal Assay Against *E. multilocularis* Metacestodes

The assay was conducted in a 24-well plate, with each well containing 4 metacestodes (diameter: 4–6 mm). H1402-NPs were diluted in deionized water and applied to metacestodes at the concentrations of 28.5 and 57.0 μM. Free H1402 was dissolved in DMSO and incubated with metacestodes at final concentration of 28.5 μM. Control wells received DMSO (0.1% v/v) only. The plate was incubated in a 5% CO_2 incubator at 37°C for 12 h. The metacestode viability was assessed microscopically at scheduled time points (1 h, 2 h, 4 h, 6 h and 12 h post-treatment). A metacestode was scored as dead when its germinal layer was collapsed and clearly peeled off from the laminated layer.[20,21]

Animals and Ethics Statement

Pathogen-free C57BL/6J mice (aged 8–10 weeks, 20 ± 2 g) and BALB/c nude mice (aged 7–8 weeks, 20 ± 2 g) were provided by Beijing Vital River Laboratory Animal Technology Co., Ltd. Animals were housed in sterilized polycarbonate cages (18 cm × 35 cm) with sawdust bedding and maintained in the animal care facility of the First Affiliated Hospital of Xinjiang Medical University under controlled conditions (22°C–25°C, 50%–60% humidity, 12:12-h [L:D] cycle). The mice were fed standard rodent chow and water *ad libitum*. The animal care and experimental procedures complied with the Chinese Laboratory Animal Administration Act 2017. The welfare of the laboratory animals followed the Guidelines for the Ethical Review of Laboratory Animal Welfare People's Republic of China National Standard GB/T

35892–20181. All animal experiments and procedures were approved by the Animal Ethics Committee of the First Affiliated Hospital of Xinjiang Medical University (approval number: IACUC201902-01). Animal studies are reported in compliance with the ARRIVE guidelines.[22]

Ex vivo Fluorescence Imaging

Female BALB/c nude mice were acclimated for one week before the experiment. All of the mice were fasted overnight for 12 h with free access to water. The animals were randomly assigned to two groups (n = 20 per group); each group was administered a single oral dose (0.2 mL) of Cy5.5-H1402-NPs solution in PBS or Cy5.5-H1402 suspension in a H_2O/DMSO (40:1) mixture at a dosage of 25 mg/kg (calculated based on the mass of H1402). At 2 h, 4 h, 6 h, 8 h, and 24 h post-administration, four mice from each group were euthanatized, and their major organs (heart, liver, lungs, spleen, and kidneys) were excised and washed with PBS three times. Ex vivo fluorescence images of the aforementioned organs were obtained using an IVIS Lumina II In Vivo Imaging System (PerkinElmer Inc., Waltham, MA, USA).

In vivo Efficacy Study in a Hepatic AE Mouse Model

The hepatic AE mouse model was established through the infection of *E. multilocularis* protoscoleces using the portal vein injection method. C57BL/6J mice were anesthetized with isoflurane in medical oxygen (4% isoflurane for induction, 1.5%–2.5% for maintenance, flow rate: 2 L/min). For analgesia, 0.15 mg/kg of buprenorphine was administered subcutaneously before and 8 h after surgery. The abdomen of the mice was shaved and sterilized with iodophor. The mice were covered with slotted sterile drapes exposing only the sterile portion of the abdomen. A 2-cm to 3-cm skin incision was made longitudinally on the abdomen, and the portal vein was exposed. A suspension of *E. multilocularis* protoscoleces (200 viable protoscoleces in 200 μL saline per mouse) was injected into the portal vein. After hemostasis, the incisions in the abdominal muscle and skin were closed using absorbable silk suture. The animals were kept on a heat pad at 38°C during recovery and were monitored every 4–6 h for 48 h following completion of the surgical procedure.

At 3 months post-infection, after confirming the growth of metacestode by ultrasonic inspection, the animals were randomly allocated into the following groups (n = 8 per group, all females): (1) unmedicated control group; (2) 100 mg/kg albendazole (ABZ) group; (3) 100 mg/kg free H1402 group; and (4) 100 mg/kg H1402-NPs group. ABZ and free H1402 were formulated in 0.5% carboxymethyl cellulose (CMC). The mice in the medicated groups were orally gavaged with 0.2 mL of the corresponding drug suspensions once daily for 30 days, while the unmedicated control animals received an equal volume of 0.5% CMC. Throughout the treatment period, mice were carefully observed for signs of emaciation, hunched back, hypoactivity, anorexia, and behavioral alterations. Uninfected control mice (n = 8) were sham-operated following the same surgical procedures as those for the infected mice except the infection of *E. multilocularis* protoscoleces, and only equal volume of saline was injected into the hepatic portal vein.

At 30 days post-treatment, all mice were anesthetized with isoflurane before collecting blood samples. Whole blood sample of each mouse was collected from the retro-orbital venous plexus. Plasma was separated by centrifugation at 2000 g for 15 min at 4°C and stored at −20°C until analysis. The mice were euthanized using CO_2 and the necropsy was conducted immediately. In the hepatic AE model, the metacestodes were embedded in the liver tissue, which could not be separated clearly; thus, the liver containing the parasite tissue of each individual was resected and weighed. The size of each metacestode on the liver surface was measured using digital image analysis software (ImageJ, Bethesda, MD, USA) to evaluate the development of metacestodes.

The hematological indices (the numbers of red blood cells [RBC], white blood cells [WBC], lymphocytes [Lym], monocytes [Mon], neutrophils [Neu], eosinophils [Eos], and basophils [Bas]), liver function (levels of alanine aminotransferase [ALT] and aspartate aminotransferase [AST]), and renal function (levels of urea nitrogen [Urea] and creatinine [Crea]) of each animal were determined using an automatic blood cell analyzer (BC-5300Vet, Mindray Bio-Medical Electronics Co., Ltd., Shenzhen, China) and a fully automatic biochemical analyzer (BS-120, Mindray Bio-Medical Electronics Co., Ltd., Shenzhen, China).

Histopathology

Histopathological analysis of liver tissue containing metacestodes was performed. Briefly, the samples from each group were fixed in 4% paraformaldehyde for 36 h and then dehydrated and embedded in paraffin. Sections were cut on an ultramicrotome (Reichert-Jung, Vienna, Austria) and stained with hematoxylin and eosin (H&E; Cat# ZLI-9610, and ZLI-9613, Zhongshan Golden Bridge Biotechnology Co., Ltd., Beijing, China). The specimens were sealed with neutral balsam and observed under a microscope (ECLIPSE Ci, Nikon Corporation, Tokyo, Japan).

Pharmacokinetic Study

The in vivo pharmacokinetic properties of H1402-NPs were investigated in BALB/c mice (aged 5–6 weeks, 20 ± 2 g, $n = 6$ per time point, three male and three female individuals were randomly assigned to per time point) following a single intravenous injection (5 mg/kg) or oral gavage (100 mg/kg). Free H1402 was dissolved in the vehicle of 5% DMSO, 10% solutol HS-15 (permeability enhancer) and 85% (20% hydroxypropyl-β-cyclodextrin in saline) for IV (5 mg/kg) and PO (100 mg/kg) administration. Blood samples were collected via tail vain at 0.08, 0.25, 0.5, 1, 2, 6, 8, 12, 24 and 48 h post-administration. Plasma samples were subsequently isolated by centrifugation at 2000 g for 15 min and prepared for analysis. The drug concentration of each sample was determined by LC–MS/MS, and pharmacokinetic parameters were analyzed using Phoenix WinNonlin 7.0 software (non-compartmental model).

Statistical Analysis

The data are expressed as mean ± SEM. Statistical analysis was performed using SPSS software (v19.0). Comparisons between two groups were performed using the Student's *t*-test. For comparisons among multiple groups, one-way analysis of variance followed by Tukey's post hoc test was conducted. Post hoc tests were run only if F achieved $p < 0.05$, and there was no significant variance inhomogeneity. In the case of heterogeneity of variance, a nonparametric Kruskal–Wallis test was conducted. A p-value < 0.05 was considered statistically significant.

Results

Characterization of PLGA-PEG-PLGA Polymers

Polymerization of PEG with GA and LA was performed through the ring-opening polymerization process (Figure S1). The polymeric nanoparticles formed in this way have an amphiphilic character with both hydrophobic and hydrophilic chains, which spontaneously form polymeric nanoparticles in aqueous solution. Nonconjugated PEG, GA, and LA were removed with a dialysis membrane. The PLGA-PEG-PLGA polymers were confirmed using ^{1}H NMR and FT-IR spectroscopy (Figure S2).

Characterization of H1402-Loaded PLGA Nanoparticles

The TEM micrograph (Figure 1) shows that the prepared H1402-NPs were homogeneously dispersed in an aqueous solution in the shape of spherical particles with a smooth surface, and the particle size was in the range of 50–60 nm. DLS analyses indicated that the average particle diameter of H1402-NPs was 55 nm (Figure 1), which is consistent with the TEM observations. The drug loading content and drug encapsulation efficiency of H1402-NPs were calculated as 8.2% and 82.1%, respectively.

Pre-Cyst Uptake

Using a near infrared dye as the fluorescent probe, the uptake of the Cy5.5-labeled H1402 nanoparticle formulation by in vitro cultured *E. multilocularis* pre-cysts was qualitatively investigated using fluorescence microscopy (Figure 2). H1402-NPs probing revealed a time-dependent uptake increase in the pre-cysts. H1402-NPs penetrated the pre-cysts rapidly and were extensively accumulated intra-cysts at only 1 h post-treatment, following which, a steady increase in cystic uptake was recorded, which plateaued at 6-h post-treatment.

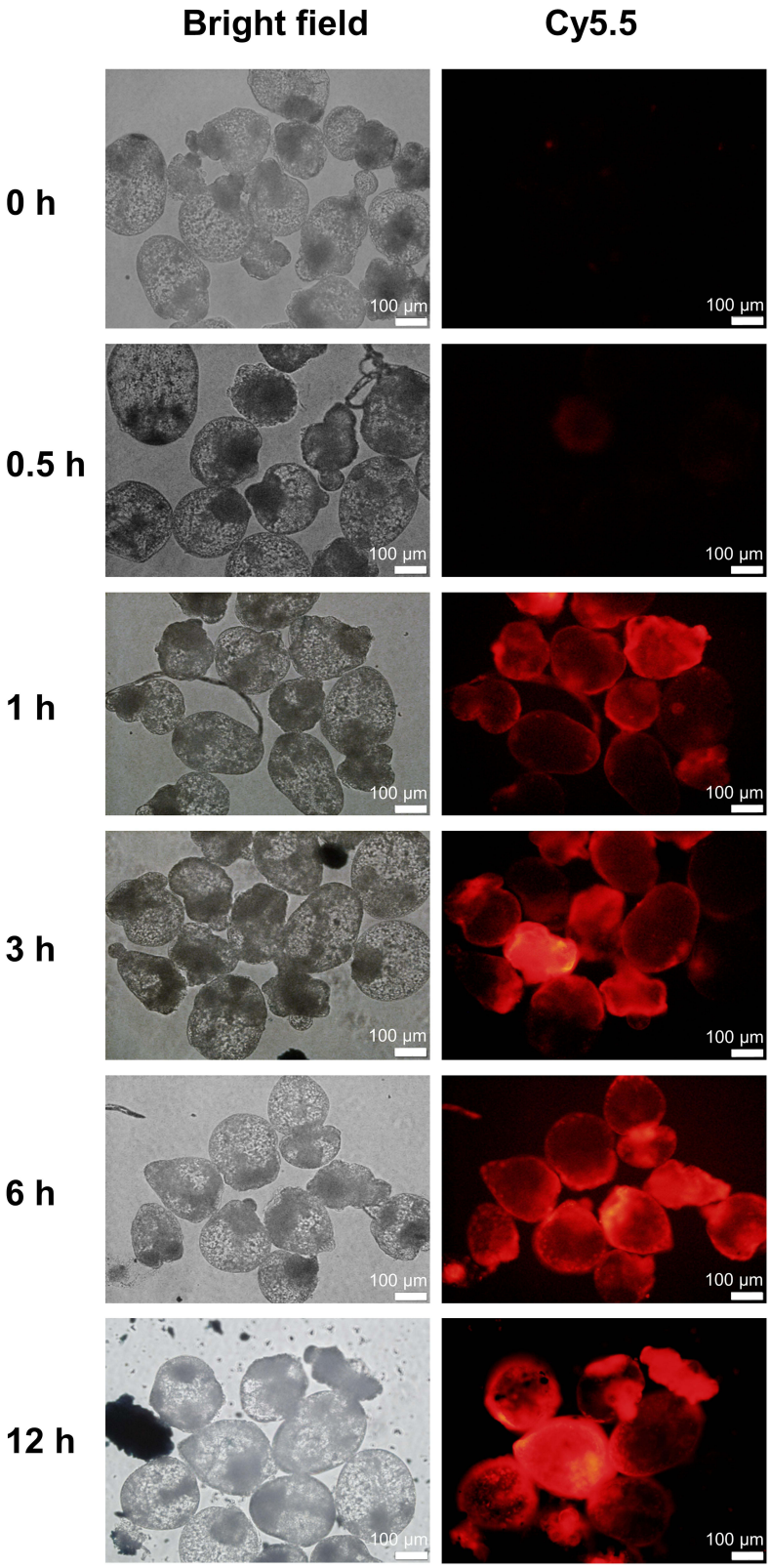

Figure 2 Uptake of Cy5.5-labeled H1402 nanoparticles by in vitro cultured *E. multilocularis* pre-cysts. The pre-cysts were incubated with H1402-NPs at a concentration of 20 μM for 12 h. Bright-field and fluorescent images are presented.

Cytotoxicity Against Human Cell Lines and Parasiticidal Activity Against *E. multilocularis* Metacestodes

Encapsulating compound H1402 into nanoparticle formulation exhibited significantly decreased cytotoxicity against human HepG2 cells. H1402-NPs revealed a negligible cytotoxic level (CC_{50} = 61.5 μM, Figure 3), which was four-fold less toxic than free H1402 (CC_{50} = 14.9 μM). Additionally, H1402-NPs exhibited potent parasiticidal activity against *E. multilocularis* metacestodes in a dose- and time-dependent manner (Figure 3). All metacestodes were killed rapidly within only 6 h at a concentration of 57.0 μM. All of the metacestodes (100%) were killed by H1402-NPs within 12 h at a concentration of 28.5 μM, with no evidence of significant cytotoxicity against human HepG2 cells at the same concentration. H1402-NPs were much less toxic against host cells than *E. multilocularis* metacestodes, indicating a potential therapeutic window.

Biodistribution of H1402 Nanoparticles in Mice

The biodistribution was visually investigated using ex vivo imaging of the major organs of healthy mice at scheduled time points after oral administration of Cy5.5-labeled free H1402 or H1402-NPs (Figure 4). H1402-NPs group exhibited the strongest fluorescence in the liver and the second strongest in the lungs within 24 h post-treatment; this indicated that most of the H1402-NPs were captured by the liver and lung tissues, which are the organs most affected by AE. For H1402-NPs-treated animals, significantly higher fluorescence intensity was observed in the liver at almost all time points across the whole observation period compared to that of the free H1402 group, which demonstrated a greater active liver-

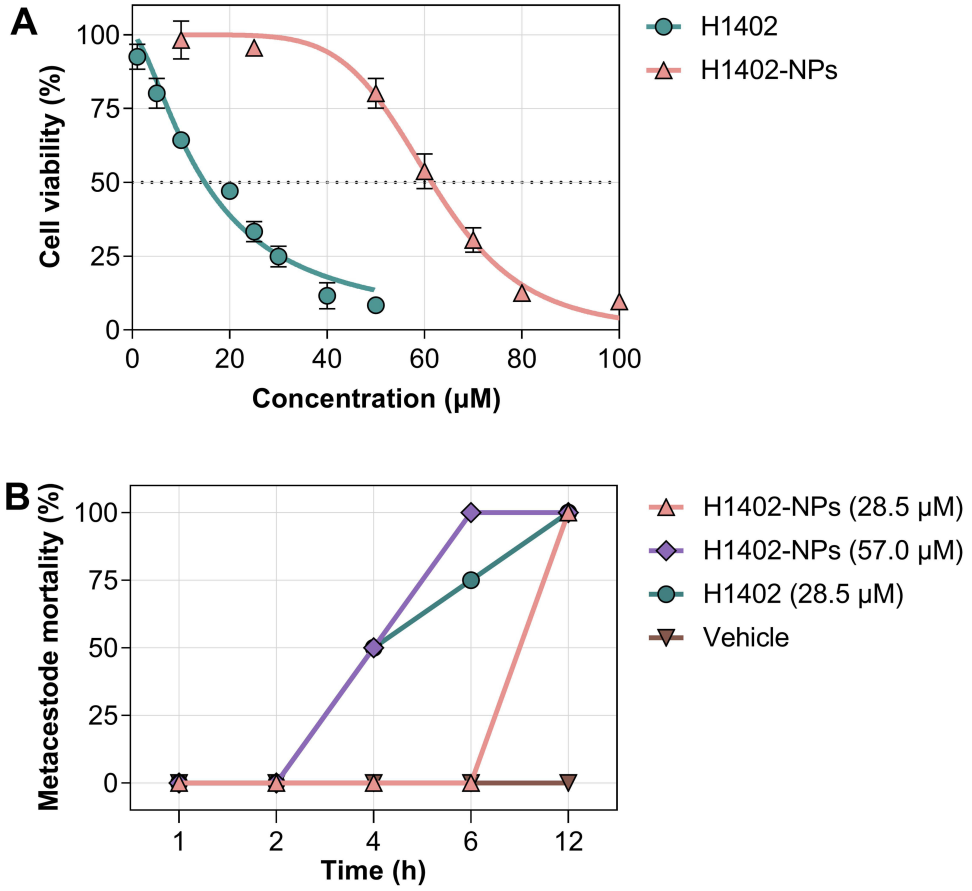

Figure 3 Cytotoxicity and parasiticidal activity against *E. multilocularis* metacestodes. (**A**) Cytotoxicity of H1402-NPs against the HepG2 cell line. HepG2 cells were treated with H1402-NPs at the indicated concentrations for 48 h. Cell viability was evaluated using the CCK-8 assay and normalized to the vehicle controls. Data are presented as the mean ± SEM. (**B**) Parasiticidal activity of H1402-NPs against in vitro cultured *E. multilocularis* metacestodes. Metacestodes were incubated with H1402-NPs at the concentrations of 28.5 and 57.0 μM for 12 h (n = 4). The metacestode mortality was assessed at the indicated time points.

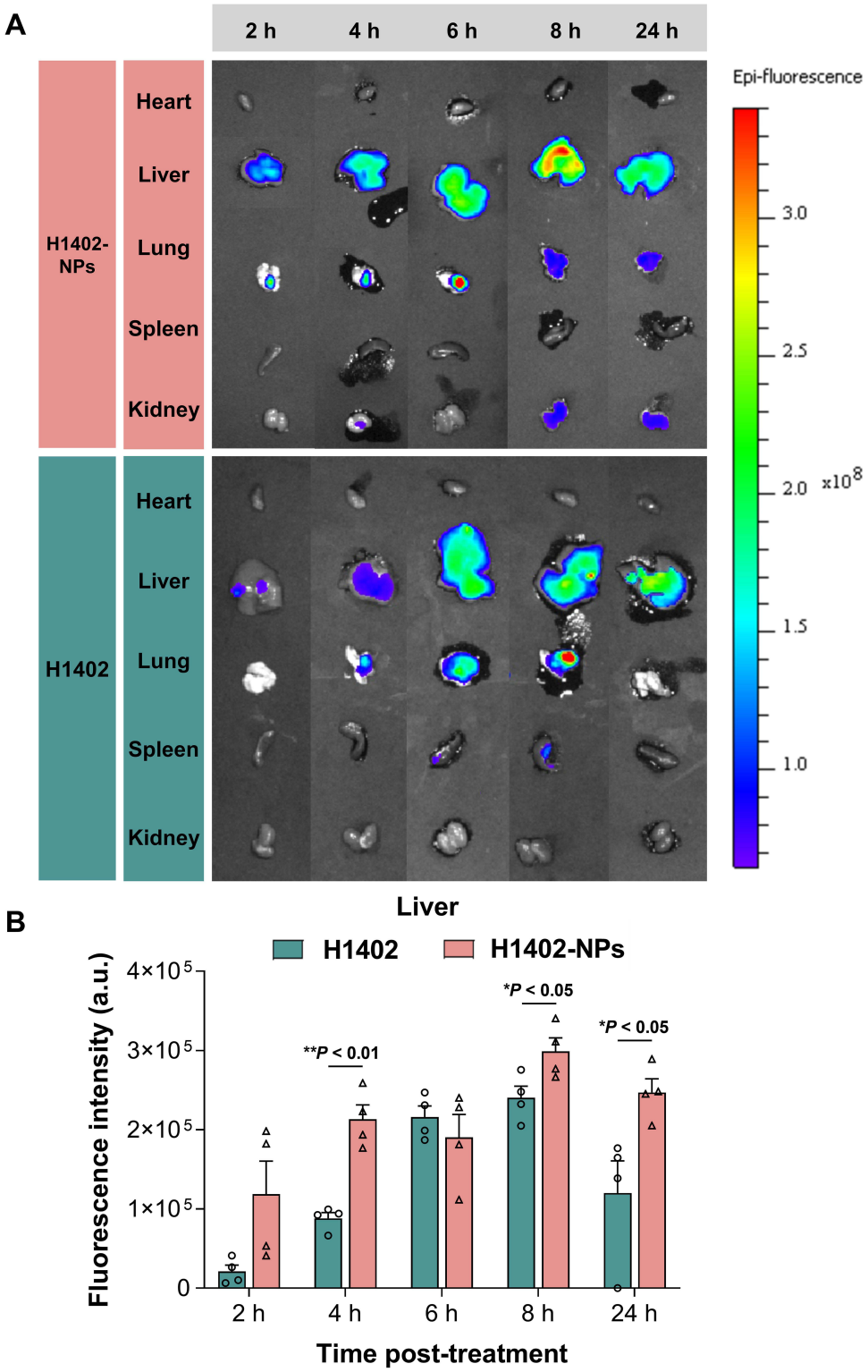

Figure 4 Biodistribution of Cy5.5-labeled free H1402 and H1402-NPs in mice following oral administration (25 mg/kg, *n* = 4 per time point). (**A**) Representative near-infrared optical images of the major organs excised at 2 h, 4 h, 6 h, 8 h, and 24 h post-administration of free H1402 and H1402-NPs. (**B**) Quantitative fluorescence intensity of liver obtained from the ex vivo images (*n* = 4). Data are presented as the mean ± SEM. **p* < 0.05; ***p* < 0.01 (*t*-test).

targeting effect of H1402-NPs. H1402-NPs accumulated rapidly in the liver a short time after administration (2 h). The concentration was sustained at a high level even at 24 h post-treatment, while the fluorescence intensity in the liver of the free H1402 group decreased rapidly, with a 49.9% decrease was observed from 8 h to 24 h. These results indicated that

the H1402-NPs had stronger liver-targeting capacity and were more effective in delivering H1402 to the liver to increase the drug retention in the parasite lesion.

Oral Administration of H1402 Nanoparticles Significantly Reduced the Parasitic Burden in a Hepatic AE Mouse Model

To mimic the natural infection and improve the clinical relevance, a hepatic *E. multilocularis* infection animal model was established and employed to evaluate the liver-targeting anti-echinococcal efficacy of H1402-NPs. In the hepatic AE model, the metacestodes were precisely developed in the liver tissue (Figure S4), and the parasitism of the *E. multilocularis* metacestodes resulted in a liver (also containing metacestodes) weight increment, indicative of the parasitic burden. As the forming metacestodes were embedded in the liver tissue and could not be separated clearly, the in vivo drug efficacy was assessed by measuring the metacestode size and liver and metacestode total weight of the infected animals. As expected, H1402-NPs were orally bioavailable and potently suppressed the growth of metacestodes as well as the dilatation of lesions (Figure 5). Oral treatment with H1402-NPs at a dosage of 100 mg/kg shrank the average metacestode size by 89.9%, showing a significant reduction compared to that of vehicle controls ($p < 0.05$) (Figure 5A). Compared to the albendazole-treated and free H1402-treated mice, the average metacestode size of the animals administered H1402-NPs was reduced by 69.1% and 40.5%, respectively, although there was no statistical difference among the three groups (Figure 5A). A significant elevation of the liver and metacestode total weight was observed in the unmedicated infected mice compared to the sham-operated individuals ($p < 0.01$), which indicated the parasitic burden of *E. multilocularis* infection. Following treatment with H1402-NPs, the liver and metacestode total weight of the infected animals was restored to normal (no significance compared to the sham group) and was significantly lower than those of the unmedicated infected mice ($p < 0.05$) and free H1402-treated mice ($p < 0.001$), demonstrating a remarkable reduction in parasitic burden (Figure 5B).

Histopathological Analysis of Hepatic *E. multilocularis* Metacestodes Following H1402 Nanoparticles Treatment

Multifocal coalescing metacestodes were observed in the livers of infected animals (Figure S4). Metacestodes were characterized by whitish, transparent, chambered, unequal-sized capsules filled with liquid. Microscopically, they were surrounded and separated by bands of connective tissue that extended into the hepatic parenchyma, thereby disrupting and replacing it. Histopathological analysis indicated intact germinal and laminated layers. Following treatment with H1402-NPs, the turgid shape of the metacestodes was lost. H1402-NPs had a pronounced effect on the germinal and laminated layers, resulting in severe degeneration and disintegration of the germinal layer, and almost complete disappearance of the laminated layer. Unlike the features of inflammatory infiltrate, fibroplastic proliferation, and hepatocellular necrosis observed in albendazole or free H1402 groups, the liver parenchyma surrounding the metacestodes was recovered very well in H1402-NPs-treated mice (Figure 5C-F).

In vivo Toxicity of H1402 Nanoparticles

Throughout the 30-day therapeutic period and 30-day recovery period, there were no significant changes in the body weight and organ weight in the H1402-NPs treatment group compared to those of shamed animals (Figure 5G), and the behavior and appearance of the mice remained normal. Moreover, no significant pathological changes in the liver, kidneys and spleen were observed in H1402-NPs-treated animals, and the hematological parameters and renal function indices (Figure 5H and I) were all within normal limits. Regarding liver function, we observed various degrees of increase in the mean ALT and AST values in ABZ- and free H1402-treated animals, but encapsulation of H1402 into PLGA nanoparticles did not result in elevation of liver transaminases compared to shamed individuals (Figure 5J).

In vivo Pharmacokinetic Study

In vivo pharmacokinetic profile of H1402-NPs was determined in mice following a single IV (5 mg/kg) or PO (100 mg/kg) dose (Figure 6 and Table 1). The apparent volume of distribution (V_z) of H1402-NPs was five-fold higher than that of free

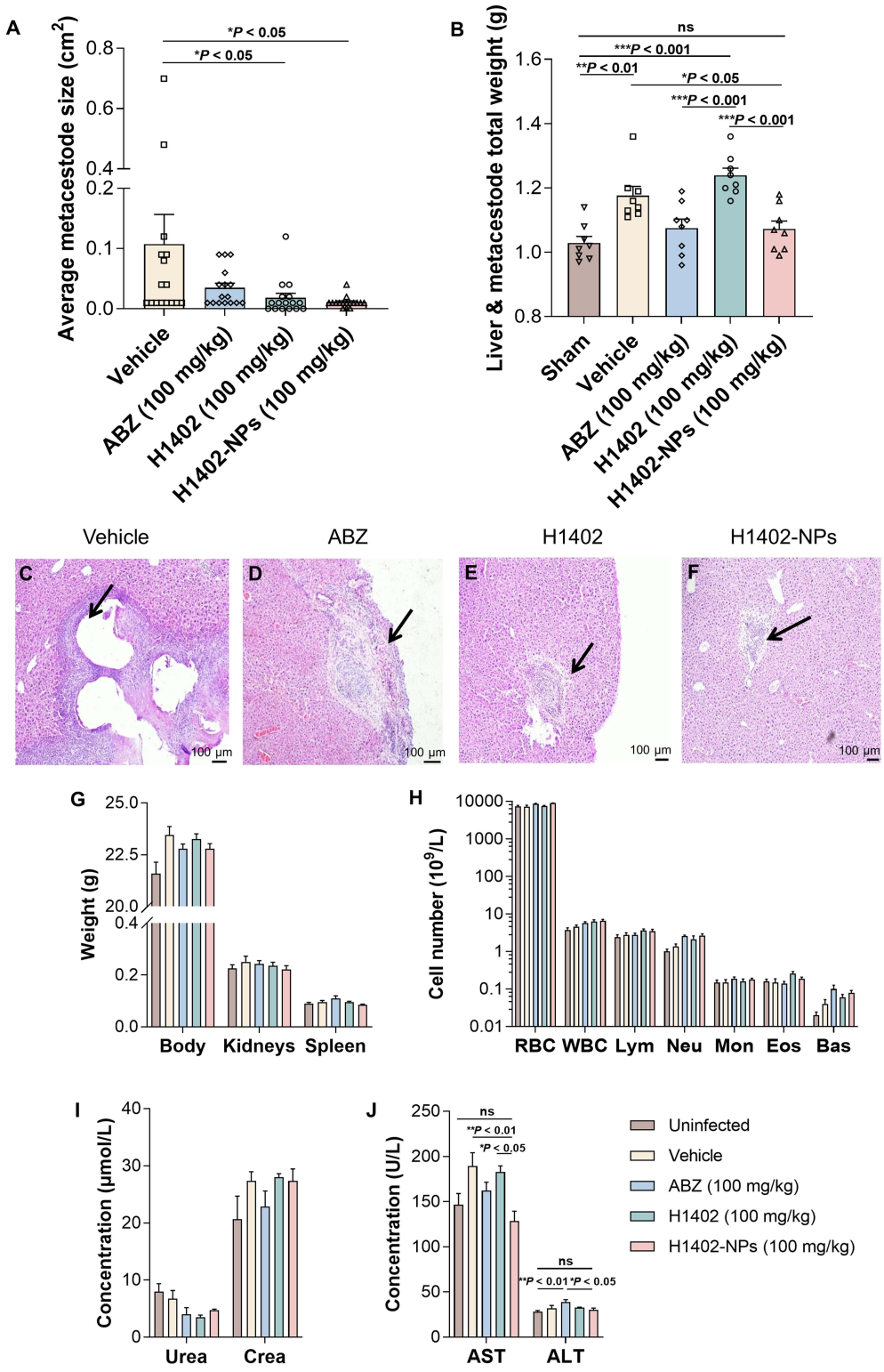

Figure 5 In vivo therapeutic efficacy and systemic toxicity of H1402 nanoparticles in a hepatic alveolar echinococcosis mouse model. The treatment groups (n = 8 for each) were orally gavaged with H1402-NPs (100 mg/kg), free H1402 (100 mg/kg), or albendazole (ABZ, 100 mg/kg) once daily for 30 days. The vehicle control (n = 8) received 0.5% carboxymethyl cellulose only. Uninfected control mice (n = 8) were sham-operated. After euthanasia, the average metacestode size (**A**) and liver and metacestode total weight (**B**) were measured. The liver tissue containing metacestodes collected from each group were stained with H&E and presented (**C-F**). The metacestodes were indicated by black arrows. The body weight and organ weight (**G**), hematological parameters (red blood cells [RBC], white blood cells [WBC], lymphocytes [Lym], monocytes [Mon], neutrophils [Neu], eosinophils [Eos], and basophils [Bas]) (**H**), renal function indices (plasma urea nitrogen [Urea] and creatinine [Crea]) (**I**), liver transaminases (aspartate aminotransferase [AST] and alanine aminotransferase [ALT]) (**J**) of mice were measured. Data are presented as the mean ± SEM. *p < 0.05; **p < 0.01; ***p < 0.001; ns: no significance (one-way analysis of variance or nonparametric Kruskal–Wallis test).

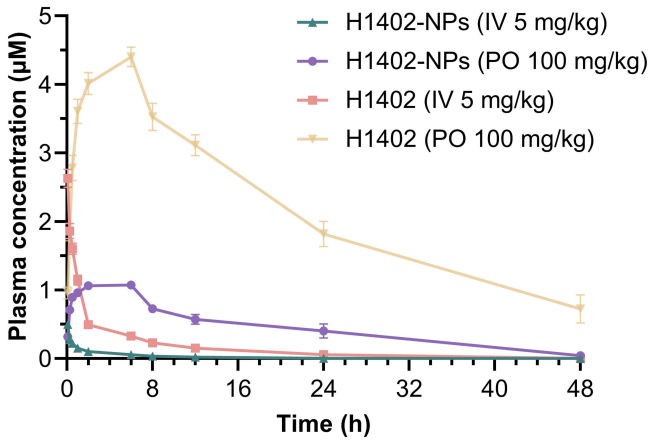

Figure 6 Plasma concentration-time profiles of H1402-NPs in mice following a single intravenous (5 mg/kg) or oral (100 mg/kg) administration. Each data point represents the mean ± SEM (n = 6 per time point).

H1402, which demonstrated that H1402-NPs were much more distributed to the organs/tissues compared with the free drug. It is consistent with the lower area under the plasma concentration-time curve (AUC) and maximal plasma concentration (C_{max}) observed in the H1402-NPs group, which could be attributable to the enhanced accumulation of nanoparticles in the liver. In addition, encapsulating H1402 into PLGA nanoparticles has gained an attention for the excellent absolute bioavailability (F) of 99.5%. Following intravenous injection, the drug elimination half-life ($T_{1/2}$) for H1402-NPs was almost identical with that of free H1402, while in the case of oral administration, the half-lives of both groups were much longer, probably due to the gender-specific elimination of H1402 in mice (free H1402: $T_{1/2\ male}$ = 10.4 h; $T_{1/2\ female}$ = 24.6 h; H1402-NPs: $T_{1/2\ male}$ = 6.4 h; $T_{1/2\ female}$ = 11.5 h).

Discussion

Human AE is an aggressive and life-threatening parasitic infection that poses a major public health issue and causes substantial socioeconomic burden in developing countries, especially in Western China.[8] Currently, the clinical treatment options for AE are limited and mainly depend on anti-parasitic drug therapy. An evaluation study in China has shown that > 70% of patients with echinococcosis received drug therapy, whereas < 7% of patients underwent surgical interventions during 2011–2016 (personal communication with Prof. Wen Hao, Xinjiang Medical University, China). So far, ABZ remains the pillar of anti-AE drugs. However, the parasitistatic rather than parasiticidal feature of ABZ determines the life-long medication, and this leads to the problems in patient compliance, high treatment costs, and elevated risk of severe adverse effects, which are the primary causes of treatment discontinuation or even failure (the resumption of parasite growth). This situation underlines the urgency of discovering and developing alternative anti-parasitic drugs against AE. However, the development of orphan drugs for the neglected disease AE is of limited interest for global

Table 1 In vivo Pharmacokinetic Profile of H1402-NPs

Parameters	H1402		H1402-NPs	
	IV (5 mg/kg)	PO (100 mg/kg)	IV (5 mg/kg)	PO (100 mg/kg)
C_{max} (μM)	2.6	4.4	0.5	1.1
T_{max} (h)	0.083	6.0	0.083	3.1
$T_{1/2}$ (h)	7.0	17.5	6.0	8.9
V_z (L/kg)	19.0	—	106.2	—
Cl (mL/min/kg)	32.0	—	207.8	—
AUC_{0-t} (h*μM)	7.5	104.4	1.1	21.7
$AUC_{0-\infty}$ (h*μM)	7.6	127.9	1.2	22.4
Oral bioavailability (F, %)	—	69.8	—	99.5

pharmaceutical companies due to economic reasons and the lack of a viable market. In the last two decades, there have been limited reports regarding new chemical entities (eg, the carbazole aminoalcohol derivative H1402) specifically developed against *E. multilocularis* infections. Moreover, although a range of clinically available drugs have been repurposed for anti-AE studies,[23–27] none of them have proceeded to clinical application. One reason for this is the unsatisfactory therapeutic efficacy caused by insufficient drug exposure in the parasite lesions (mainly the liver). Therefore, in this work, we hypothesized that the novel parasiticidal rather than parasitistatic anti-echinococcal agent H1402 developed with a liver-targeting drug delivery system would produce enhanced therapeutic outcomes against *E. multilocularis* infections.

Carbazole alkaloid, as a privileged structure in medicinal chemistry, has been widely reported to have extensive biological activities including antimicrobial, antitumor, antiviral and anti-Alzheimer.[28–31] In the previous studies, we designed and synthesized a series of carbazole aminoalcohol derivatives (one representative is H1402), which exhibited broad-spectrum anti-parasitic activities against *Echinococcus* and *Trypanozoon* in vitro and in vivo,[15,16,32] and *Plasmodium* and *Schistosoma* in vitro.[33] Especially significant therapeutic efficacy was achieved following the oral treatments of the carbazole aminoalcohols in mice infected with *E. granulosus s.l.*, while unfortunately the anti-parasitic potency declined for AE.

Learned from the lessons of ABZ, low bioavailability in both in plasma and intra-cysts compromises the anti-echinococcal therapeutic efficacy.[34,35] An ideal anti-AE agent should have a favorable pharmacokinetic profile to reach a sufficient concentration at the parasitized organs/tissues and at intra-cystic levels to trigger an effective anti-parasitic response. However, as a small molecular compound, the whole-body biodistribution and cellular uptake of H1402 commonly depends on passive diffusion, which may be inadequate for the coalescing and invasive *E. multilocularis* metacestodes. In both academia and industry, copolymers containing PLGA and PEG blocks are attracting great interest for drug delivery systems and biomedical applications due to their biodegradable nature and biocompatible properties.[36,37] Ex vivo fluorescence imaging showed that encapsulating compound H1402 into PLGA nanoparticles altered the intrinsic biodistribution profile of the drug and effectively delivered compound H1402 to the liver, where the metacestodes predominantly parasitize. The high concentration of the drug accumulated around the AE lesion is assuredly beneficial for drug uptake and important for killing the inner parasites. Additionally, the small size (< 100 nm) and spherical shape of H1402-NPs are favorable to be internalized by metacestodes via non-specific endocytosis or other passive pathways.[38] Moreover, both routes of internalization are affected by the concentration of drug around the lesion and would generate profits from the high accumulation of the drug in the liver. Our in vitro uptake assay results demonstrated that, with the mediation of PLGA-PEG-PLGA polymeric nanocarrier, H1402 could rapidly penetrate through the pre-cyst wall, extensively accumulate within the in vitro cultured pre-cysts, and effectively kill them, indicating that nanoparticle formulation could promote the drug uptake and improve the intra-cystic content of H1402. This high cystic uptake or increased intra-cystic drug concentration was also noted in ABZ- or fenbendazole-encapsulated nanoparticles for treating AE/CE in previous studies.[39,40]

The maintenance of drug bioactivity after encapsulation is a prerequisite for a nanocarrier. The in vitro anti-parasitic study revealed that H1402-NPs could kill *E. multilocularis* metacestodes potently and rapidly. Although there is a tiny gap to free H1402, H1402-NPs still exhibited much stronger potency than ABZ (no non-viable metacestodes at a concentration of 30 μM following 24-h treatment), which is likely attributed to the parasiticidal characteristic of compound H1402. However, considering that PLGA nanoparticles usually exhibit a prolonged and sustained release pattern, the in vitro anti-metacestode ability of H1402-NPs might be underestimated.

Currently, the most commonly used in vivo AE rodent models are based on the experimentally-induced development of the parasite after intraperitoneal injection of viable *E. multilocularis* metacestode suspensions (secondary infection).[41] The development of the parasite within the peritoneal cavity of secondarily infected animals has some limitations when attempting to reproduce a natural infection in the intermediate host of *E. multilocularis*, as the parasitized site of primary infection is usually the liver. It should also be noted that there are variations in terms of therapeutic efficacy of systemic drug treatments for the metacestodes located in different locations (eg, intraperitoneal or intraparenchymatous).[34] Differences in drug concentrations in tissues and/or drug exposure should be also considered. In this context, to mimic the features of *E. multilocularis* primary infection as much as possible, we have established a hepatic AE

mouse model through the portal vein infection of protoscoleces, where the metacestodes are precisely developed in the liver tissue.

Except for intravenous administration, few other (especially non-invasive) administration methods have been reportedly applied for drug-loaded PLGA NPs; this is an inconvenience to patients affected by chronic diseases and requires multiple dosing. In this work, we employed a long-term oral gavage administration as an extended delivery system for H1402-loaded PLGA NPs to treat chronic, complicated, and difficult-to-treat AE. The design of the oral administration dosage of H1402-NPs referenced the recommended average dosage of ABZ for humans (10–15 mg/kg/day) in clinical practice, which is equivalent in mice to 123–184.5 mg/kg/day according to the human-animals equivalent dose formula.[42] Combined with our previous experience, the dosage of 100 mg/kg/day was employed by H1402-NPs in this work, as that used to treat *E. granulosus s.l.*-infected mice in our previous study,[15] and was compared to ABZ at the same dosage. The 30-day oral regimen of 100 mg/kg/day H1402-NPs exhibited great therapeutic effects in the hepatic AE mouse model, achieving a significant reduction both in the parasite mass (liver and metacestode total weight, 8.8%) and average metacestode size (89.9%) compared to unmedicated infected mice (both p-values < 0.05), which was slightly more active than the ABZ treatment (100 mg/kg/day). Although following the same regimen, the treatment outcome of free H1402 against AE was less effective as that observed in an intraperitoneally infected CE mouse model and only significantly reduced the average metacestode size but not the parasite weight; this was likely due to the complex and aggressive characteristics of AE and the influence of intraperitoneal or intraparenchymatous parasite lesions. Encapsulating H1402 into the nanoparticle formulation significantly improved the anti-parasitic effectiveness in terms of the reduction in parasite weight compared to free H1402 ($p < 0.001$). Notably, the liver and metacestode total weight of the H1402-NPs group was almost restored to the normal level of shamed animals ($p > 0.05$), suggesting a strong clinical impact of this novel drug formulation. The powerful parasiticidal ability was further confirmed by the devastating damage to metacestode tissues observed microscopically. The enhanced efficacy of H1402-NPs could be attributed to the liver-targeting effect and continued particle delivery into the metacestodes, resulting in effective bioavailability and longer retention of the drug in the target organ and intra-cysts.

Importantly, an ideal anti-parasitic agent for AE treatment should be selectively toxic against the parasite but not the host. The cytotoxicity of free H1402 against human liver cells was significantly reduced after PLGA-PEG-PLGA NP encapsulation. In H1402-NPs-treated cells, the cell viability was sustained, even at high concentrations of the drug, suggesting that the reduced toxicity could be related to the progressive release of H1402 from the nanocarrier. Hepatic *E. multilocularis* infection and/or long-term anti-parasitic drug treatment usually result in liver lesions and a typical manifestation is the elevated levels of liver transaminase.[43,44] Additionally, evidence has shown that nanoparticles are preferentially deposited in the liver under systemic exposure, resulting in prolonged retention within the organ and, in some instances, significant hepatotoxicity. Thus, the potential adverse effects of the 30-day regimen of H1402-NPs on the liver was one of our concerns. Our in vivo studies showed a real increase in the serum transaminase levels (either AST or ALT) among those mice in the ABZ-, H1402-, and vehicle-treated groups, which did not occur in the H1402-NPs group of animals where levels remained normal. The results were further confirmed by the fact that no obvious histopathological changes or injuries were observed in the liver tissue. Furthermore, in vivo safety assessment revealed that the H1402-NPs treatment did not induce unwanted systemic toxicity in mice. Throughout the treatment, the behavior and appearance of the mice were normal and no significant pathological changes were observed in the major organs. The hematological parameters and biochemical indices were all within normal limits.

Despite the encouraging results derived from this study, some limitations were observed during its development. First, the intra-cystic concentration range and retention period of H1402-NPs warrant consideration given that the cyst fluid may not be the same as the body fluid in a systemic physiological environment. Investigation into the intra-cystic drug-release pattern could be performed to clarify this issue. Second, although the hepatic AE mouse model employed in this study showed substantial superiority to the conventional intraperitoneal infection model, the anti-AE efficacy in naturally infected hosts is difficult to predict. Further studies conducted in suitable primarily infected animals will greatly strengthen the clinical impact of H1402-NPs. Additionally, the elected time point to initiate the drug regimen is of importance for treatment outcome,[45,46] The regimens started on day 0, and 3- or 6-months post-infection would be appropriate to investigate the chemoprophylactic effect or therapeutic efficacy against early-stage or late-stage infection.

Finally, we expect that an integrated therapeutic strategy through employing a combinational nanoformulation of two drugs with different mechanisms of action (eg, H1402 combined with a known anti-AE agent, an immunomodulator or a liver-protective drug) would produce synergistic anti-AE benefits, allowing a significant enhancement of their individual therapeutic performances or a reduction of daily administration dosage of one or both drugs. Investigations into H1402/ABZ-co-encapsulated nanoparticle combination therapy are in progress.

Conclusion

Considering the findings of this study, we conclude that encapsulating H1402 into a PLGA-PEG-PLGA nanoformulation efficiently delivered the parent drug to the liver and facilitated extensive accumulation in the parasite tissue. More importantly, in vivo therapeutic efficacy studies demonstrated that H1402-NPs achieved remarkably improved anti-AE treatment outcomes together with reduced systemic toxicity compared to free H1402 or ABZ. Taken together, H1402-NPs, as a nanodrug, possess additional advantages, including a new chemotype, approved nanocarrier materials, high cystic uptake, satisfactory safety profile, and, in particular, profound performance in liver targeting, and represent a promising therapeutic strategy for hepatic AE.

Acknowledgments

This work was supported by the National Natural Science Foundation of China (grant numbers 81830066, 32072886, U1803282 and 82161148008); Clinical Research Project of Healthcare Industry of Shanghai Municipal Health Commission (grant number 202040054); 2021 Kunlun Talents Project-High-Level Innovative and Entrepreneurial Talents; and Natural Science Foundation of Qinghai Province (grant number 2021-ZJ-933).

Disclosure

The authors report no conflicts of interest in this work.

References

1. Wen H, Vuitton L, Tuxun T, et al. Echinococcosis: advances in the 21st Century. *Clin Microbiol Rev*. 2019;32(2):e00075_18.
2. Torgerson PR, Devleesschauwer B, Praet N, et al. World Health Organization Estimates of the Global and Regional Disease Burden of 11 Foodborne Parasitic Diseases, 2010: a Data Synthesis. *PLoS Med*. 2015;12(12):e1001920.
3. Wu W, Wang H, Wang Q, et al. A nationwide sampling survey on echinococcosis in China during 2012-2016 (in Chinese). *Chine J Parasitol Parasitic Dis*. 2018;36(1):1–14.
4. Torgerson PR, Keller K, Magnotta M, Ragland N, Brooker S. The global burden of alveolar echinococcosis. *PLoS Negl Trop Dis*. 2010;4(6):e722.
5. Budke CM, Jiamin Q, Zinsstag J, Qian W, Torgerson PR. Use of disability adjusted life years in the estimation of the disease burden of echinococcosis for a high endemic region of the Tibetan plateau. *Am J Trop Med Hyg*. 2004;71(1):56–64.
6. Vuitton DA, Demonmerot F, Knapp J, et al. Clinical epidemiology of human AE in Europe. *Vet Parasitol*. 2015;213(3–4):110–120.
7. Gottstein B, Stojkovic M, Vuitton DA, Millon L, Marcinkute A, Deplazes P. Threat of alveolar echinococcosis to public health–a challenge for Europe. *Trends Parasitol*. 2015;31(9):407–412.
8. Kern P, Menezes Da Silva A, Akhan O, et al. The Echinococcoses: diagnosis, clinical management and burden of disease. *Adv Parasitol*. 2017;96:259–369.
9. McManus DP, Gray DJ, Zhang W, Yang Y. Diagnosis, treatment, and management of echinococcosis. *BMJ*. 2012;344:e3866.
10. Gruner B, Kern P, Mayer B, et al. Comprehensive diagnosis and treatment of alveolar echinococcosis: a single-center, long-term observational study of 312 patients in Germany. *GMS Infect Dis*. 2017;5:Doc1.
11. Hemphill A, Stadelmann B, Rufener R, et al. Treatment of echinococcosis: albendazole and mebendazole--what else? *Parasite*. 2014;21:70.
12. Lundstrom-Stadelmann B, Rufener R, Ritler D, Zurbriggen R, Hemphill A. The importance of being parasiticidal. an update on drug development for the treatment of alveolar echinococcosis. *Food Waterborne Parasitol*. 2019;15:e00040.
13. Reuter S, Buck A, Manfras B, et al. Structured treatment interruption in patients with alveolar echinococcosis. *Hepatology*. 2004;39(2):509–517.
14. Steiger U, Cotting J, Reichen J. Albendazole treatment of echinococcosis in humans: effects on microsomal metabolism and drug tolerance. *Clin Pharmacol Ther*. 1990;47(3):347–353.
15. Wang W, Li J, Yao J, et al. In vitro and in vivo efficacies of novel carbazole aminoalcohols in the treatment of cystic echinococcosis. *J Antimicrob Chemother*. 2017;72(11):3122–3130.
16. Dang Z, Xu S, Zhang H, et al. In vitro and in vivo efficacies of carbazole aminoalcohols in the treatment of alveolar echinococcosis. *Acta Trop*. 2018;185:138–143.
17. Lin T, Gao DY, Liu YC, et al. Development and characterization of sorafenib-loaded PLGA nanoparticles for the systemic treatment of liver fibrosis. *J Control Release*. 2016;221:62–70.
18. Chen XP, Li Y, Zhang Y, Li GW. Formulation, characterization and evaluation of curcumin-loaded PLGA-TPGS nanoparticles for liver cancer treatment. *Drug Des Devel Ther*. 2019;13:3569–3578.

19. Kurniawan DW, Jajoriya AK, Dhawan G, et al. Therapeutic inhibition of spleen tyrosine kinase in inflammatory macrophages using PLGA nanoparticles for the treatment of non-alcoholic steatohepatitis. *J Control Release*. 2018;288:227–238.
20. Li J, Wang W, Yao J, et al. Old drug repurposing for neglected disease: pyronaridine as a promising candidate for the treatment of Echinococcus granulosus infections. *EBioMedicine*. 2020;54:102711.
21. Lopez LM, Pensel PE, Fabbri J, et al. The combination of carvacrol and albendazole enhanced the efficacy of monotherapy in experimental alveolar echinococcosis. *Acta Trop*. 2022;225:106198.
22. du Sert NP, Hurst V, Ahluwalia A, et al. The ARRIVE guidelines 2.0: updated guidelines for reporting animal research. *PLoS Biol*. 2020;18(7):e3000410.
23. Enkai S, Kouguchi H, Inaoka DK, Irie T, Yagi K, Kita K. In vivo efficacy of combination therapy with albendazole and atovaquone against primary hydatid cysts in mice. *Eur J Clin Microbiol Infect Dis*. 2021;40(9):1815–1820.
24. Liu C, Fan H, Ma J, Ma L, Ge RL. In vitro and in vivo efficacy of thiacloprid against Echinococcus multilocularis. *Parasit Vectors*. 2021;14(1):450.
25. Joekel DE, Lundstrom-Stadelmann B, Mullhaupt B, Hemphill A, Deplazes P. Evaluation of kinase-inhibitors nilotinib and everolimus against alveolar echinococcosis in vitro and in a mouse model. *Exp Parasitol*. 2018;188:65–72.
26. Rufener R, Ritler D, Zielinski J, et al. Activity of mefloquine and mefloquine derivatives against Echinococcus multilocularis. *Int J Parasitol Drugs Drug Resist*. 2018;8(2):331–340.
27. Rufener R, Dick L, D'Ascoli L, et al. Repurposing of an old drug: in vitro and in vivo efficacies of buparvaquone against Echinococcus multilocularis. *Int J Parasitol Drugs Drug Resist*. 2018;8(3):440–450.
28. Wang G, Sun S, Guo H. Current status of carbazole hybrids as anticancer agents. *Eur J Med Chem*. 2022;229:113999.
29. Patil SA, Patil SA, Ble-González EA, Isbel SR, Hampton SM, Bugarin A. Carbazole derivatives as potential antimicrobial agents. *Molecules*. 2022;27(19):6575.
30. Tsutsumi LS, Gundisch D, Sun D. Carbazole Scaffold in Medicinal Chemistry and Natural Products: a Review from 2010-2015. *Curr Top Med Chem*. 2016;16(11):1290–1313.
31. Caruso A, Ceramella J, Iacopetta D, et al. Carbazole derivatives as antiviral agents: an overview. *Molecules*. 2019;24(10):1912.
32. Cai X, Wang W, Lai D, et al. Identification of an orally active carbazole aminoalcohol derivative with broad-spectrum anti-animal trypanosomiasis activity. *Acta Trop*. 2021;219:105919.
33. Wang W, Li Q, Wei Y, et al. Novel carbazole aminoalcohols as inhibitors of beta-hematin formation: antiplasmodial and antischistosomal activities. *Int J Parasitol Drugs Drug Resist*. 2017;7(2):191–199.
34. Siles-Lucas M, Casulli A, Cirilli R, Carmena D. Progress in the pharmacological treatment of human cystic and alveolar echinococcosis: compounds and therapeutic targets. *PLoS Negl Trop Dis*. 2018;12(4):e0006422.
35. Skuhala T, Trkulja V, Runje M, Vukelic D, Desnica B. Albendazolesulphoxide concentrations in plasma and hydatid cyst and prediction of parasitological and clinical outcomes in patients with liver hydatidosis caused by Echinococcus granulosus. *Croat Med J*. 2014;55(2):146–155.
36. Mir M, Ahmed N, Rehman AU. Recent applications of PLGA based nanostructures in drug delivery. *Colloids Surf B Biointerfaces*. 2017;159:217–231.
37. Almoustafa HA, Alshawsh MA, Chik Z. Technical aspects of preparing PEG-PLGA nanoparticles as carrier for chemotherapeutic agents by nanoprecipitation method. *Int J Pharm*. 2017;533(1):275–284.
38. Oh N, Park JH. Endocytosis and exocytosis of nanoparticles in mammalian cells. *Int J Nanomedicine*. 2014;9(Suppl 1):51–63.
39. Liu Y, Wang XQ, Ren WX, et al. Novel albendazole-chitosan nanoparticles for intestinal absorption enhancement and hepatic targeting improvement in rats. *J Biomed Mater Res B Appl Biomater*. 2013;101(6):998–1005.
40. Farhadi M, Haniloo A, Rostamizadeh K, Faghihzadeh S. Efficiency of flubendazole-loaded mPEG-PCL nanoparticles: a promising formulation against the protoscoleces and cysts of Echinococcus granulosus. *Acta Trop*. 2018;187:190–200.
41. Hemphill A, Stadelmann B, Scholl S, et al. Echinococcus metacestodes as laboratory models for the screening of drugs against cestodes and trematodes. *Parasitology*. 2010;137(3):569–587.
42. Nair AB, Jacob S. A simple practice guide for dose conversion between animals and human. *J Basic Clin Pharm*. 2016;7(2):27–31.
43. Li H, Song T, Shao Y, Tuergan A, Ran B, Wen H. Chemotherapy in alveolar echinococcosis of multi-organs: what's the role? *Parasitol Res*. 2013;112(6):2237–2243.
44. Karabulut K, Ozbalci GS, Kesicioglu T, et al. Long-term outcomes of intraoperative and perioperative albendazole treatment in hepatic hydatidosis: single center experience. *Ann Surg Treat Res*. 2014;87(2):61–65.
45. Nicolao MC, Elissondo MC, Denegri GM, Goya AB, Cumino AC. In vitro and in vivo effects of tamoxifen against larval stage Echinococcus granulosus. *Antimicrob Agents Chemother*. 2014;58(9):5146–5154.
46. Pensel P, Paredes A, Albani CM, et al. Albendazole nanocrystals in experimental alveolar echinococcosis: enhanced chemoprophylactic and clinical efficacy in infected mice. *Vet Parasitol*. 2018;251:78–84.

International Journal of Nanomedicine Dovepress

Publish your work in this journal

The International Journal of Nanomedicine is an international, peer-reviewed journal focusing on the application of nanotechnology in diagnostics, therapeutics, and drug delivery systems throughout the biomedical field. This journal is indexed on PubMed Central, MedLine, CAS, SciSearch®, Current Contents®/Clinical Medicine, Journal Citation Reports/Science Edition, EMBase, Scopus and the Elsevier Bibliographic databases. The manuscript management system is completely online and includes a very quick and fair peer-review system, which is all easy to use. Visit http://www.dovepress.com/testimonials.php to read real quotes from published authors.

Submit your manuscript here: https://www.dovepress.com/international-journal-of-nanomedicine-journal